Hindawi
International Journal of Aerospace Engineering
Volume 2021, Article ID 8898796, 14 pages
https://doi.org/10.1155/2021/8898796

Research Article

Effect of Negative Valve Overlap on Combustion and Emissions of CNG-Fueled HCCI Engine with Hydrogen Addition

Yuelin Li,[1] **Zihan Zhang**,[1,2] **Zhiqiang Liu**,[1] **Peng Tong**,[1,3] **Dezhi Yang**,[1] **and Wulong Zhang**[1]

[1]*College of Automotive and Mechanical Engineering, Changsha University of Science and Technology, Changsha 410114, China*
[2]*Yichun Vocational Technical College, Yichun 336000, China*
[3]*Loudi Vocational and Technical College, Loudi 417000, China*

Correspondence should be addressed to Zhiqiang Liu; lzq0228@126.com

Received 11 September 2020; Revised 17 December 2020; Accepted 20 January 2021; Published 10 February 2021

Academic Editor: William Ling

In order to study the effect of negative valve overlap on combustion and emission characteristics of a homogeneous charge compression ignition engine fueled with natural gas and hydrogen, the test and the simulation were conducted using an engine cycle model coupling the chemical kinetic reaction mechanism under different valve timing conditions. Results show that the internal EGR formed by using negative valve overlap could heat the inlet mixtures and improve the spontaneous ignition characteristic of the engine. The residual exhaust gas could slow down the heat release rate, decrease the pressure rise rate and the maximum combustion temperature, and reduce the NO_x emission simultaneously. Among the three NVO schemes, the strategy of changing the intake valve opening timing individually can create the least power loss, and the symmetric NVO strategy which changes both the exhaust valve closing timing and the intake valve opening timing simultaneously can achieve the best heating effect of inlet mixtures and the satisfactory decrease of combustion temperature, as well as the largest reduction of NO_x emission.

1. Introduction

Hydrogen fueled with natural gas (HCNG) engine is a widely studied hybrid fuel power machine, which combines the advantages of abundant resources of natural gas and fast combustion rate, wide flammability limit, and short quenching distance of hydrogen [1–3]. Researches show that the laminar flame propagation speed of hydrogen is generally higher than that of hydrocarbon fuels, and the hydroxyl radical (OH) generated by its combustion can accelerate the oxidation reaction of natural gas [4], thus making up for the shortcoming of slow combustion speed of natural gas and making the mixed combustion closer to isovolumetric heat release [5]. When HCNG is applied to compression ignition mode, the addition of hydrogen could advance the spontaneous ignition time of natural gas, broaden its flammable limit, and help to realize lean combustion [6, 7]. Some scholars have conducted relevant experiments and simulation studies on HCNG-fueled spark ignition engines, and results show that CO_2 and HC emissions are declined because hydrogen does not contain carbon, and the quenching distance of hydrogen is short [8–10]. The intermediate formaldehyde emission is rapidly consumed due to the increased activity of O and OH groups after hydrogen was added [11, 12]. At the same time, however, on account of the increase of mixed combustion rate, the maximum temperature increases and thereby leading to the increase of NO_x emission [13].

Homogeneous charge compression ignition (HCCI) has the characteristics of multipoint simultaneous ignition and rapid combustion [14], which could shorten the combustion duration and the after-combustion period [15], increase thermal efficiency, and improve fuel economy. However, the large pressure rise rate caused by fast heat transfer will

cause the engine rough running and knocking [16]. There is an urgent need to use various methods and develop new working strategies to study the combustion process of HCCI. Yousefi et al. [17] carried out a simulation adopting a coupled AVL-CHEMKIN CFD model to compare combustion phasing, engine performance, and emissions in terms of equivalence ratio for both HCCI combustion engines with and without precombustion chamber, and results revealed that HCCI engine with modified chamber has higher combustion pressure, narrower heat release rate, generates higher work per kilogram fuel, and both carbon monoxide and hydrocarbon emissions decreased, while a high level of nitrogen oxide emissions is produced by HCCI combustion. Neshat and Saray [18] developed a new four-zone combustion model for HCCI engine to predict the in-cylinder pressure and emissions, and results revealed that the implementation of accurate mass transfer model caused to accurate prediction of UHC and CO, and near zero NO_x, which is lower than 10 ppm for all of examined cases, is also predicted well. Studies show that the success of any simulation model in describing or predicting the HCCI combustion process and emission formation evidently depends partly on its ability to reliably predict the heat transfer phenomena involved, because the heat transfer process directly affects mean gas and local temperatures, thereby influencing ignition timing, combustion rate, and the formation of HC, CO, and NO_x emissions [19, 20].

In order to alleviate the heat release process of HCCI combustion, lean combustion, low temperature combustion, and variable valve timing are usually used [21]. The octane number of natural gas is very high, and in order to ensure the achievement of compression autoignition, it is required that the in-cylinder temperature is conducive to the occurrence of autoignition [22]. It is a feasible scheme to recycle high-temperature exhaust gas (EGR). The addition of exhaust gas can increase the initial temperature of intake air and accelerate the low activation energy reaction of working fluid. Because the exhaust gas is mostly H_2O, CO_2, and other gases with larger specific heat capacity, it can also dilute the fresh working fluid, suppress the heat release rate, and reduce the temperature, thus alleviating the rough combustion phenomenon and expanding the upper load limitation of HCCI combustion, and at the same time, it is beneficial to realize low-temperature combustion and reduce the heat transfer loss of combustion chamber wall [23]. The research shows that the residual active groups in the high temperature exhaust gas have a positive influence on spontaneous combustion [24]. The internal EGR formed by changing the valve timing is simpler than the external EGR with control valve. The negative valve overlap (NVO) formed by early closing of the exhaust valve and delayed opening of the intake valve can intercept the exhaust gas in the cylinder, and the EGR effect can be produced by heating and diluting the new gas during the gas exchange process. Relevant researches show that HCCI combustion with negative valve overlap can achieve a wide load range and improve high-load combustion [25]. Some scholars believe that the ideal necessary condition for HCCI is internal EGR [26], because the working fluid is easier to ignite spontaneously in EGR-rich region when the residual exhaust gas and new gas are mixed initially, and the stratified state of exhaust gas and new gas formed by NVO has the most favorable influence on HCCI ignition. Based on the contemporary reviews, it is found that previous relevant studies are mostly working on the simplification of mechanism of pure CNG or pure H_2 in HCCI engines, the basic engine performance simulation, and the characteristics of HCNG-fueled SI engines [18, 27–29], and little progress has been made in concerning the influence of negative valve overlap formed by changing valve timing on HCCI engine fueled by HCNG binary mixed fuel.

In this paper, combined with the experimental study of hydrogen fueled with natural gas engine, the numerical simulation of HCCI engine under NVO strategy is carried out on the GT-Power software and the CHEMKIN software, and the influence of changing valve timing on combustion and emission characteristics of engine is explored. By comparing three strategies, the different improvements of NVO on the working process of the engine are summarized, which provide a theoretical basis for improving the performance of natural gas-hydrogen HCCI engine in practical application.

2. Model and Numerical Method

The main research problem of HCNG fuel HCCI combustion combined with NVO is to determine the advantages and disadvantages of various valve timing schemes. However, the change of valve timing will inevitably increase the complexity of engine structure, so it is more suitable to construct suitable simulation model than test. Considering that the GT-Power software which contains the 1-D engine cycle model could simulate the gas exchange process well, and CHEMKIN has higher simulation accuracy for combustion process especially the HCCI combustion, they are selected for coupling simulation. Firstly, the relevant environmental parameters and the initial data of the engine working process are collected through experiments, the valve lift curves under different NVO strategies are imported into GT-Power, the combustion cycle model is defined, the cycle temperature and pressure curves including the gas exchange process are obtained, and various parameter values at the end of the gas exchange process are used as the initial conditions of CHEMKIN simulation. Then, the reaction mechanism and thermodynamic data of HCNG fuel are inputted into CHEMKIN, and the reaction equation required by the chemical solver is specified. Finally, the whole set of control equations of the zero-dimensional single-zone model is solved by combining the combustion model with the heat transfer model, the cylinder geometry model, and the calculation formula of EGR rate under specific NVO strategy, so that the parameters such as combustion heat release rate, in-cylinder pressure changes, and concentration of various reaction products are obtained. It is worth noting that the parameters at the end of the gas exchange process obtained in the first cycle are derived from the combustion model in GT-Power, in the subsequent cycles, the data obtained by CHEMKIN combustion process simulation will be imported back to GT-Power, so there are alternating effects between the gas exchange period and combustion process in different cycles. Therefore, iterative convergence calculation and model

parameter correction should be carried out on the parameters that determine the combustion model in combination with the experimental data so as to obtain simulation results that can better express the real situation.

2.1. Mechanism and Physical Parameters. GRI Mech-3.0 [30] describes the chemical kinetic mechanism of methane combustion oxidation reaction, including 53 substances and 325 elementary reactions, such as C1-C2 chain reaction, N chemical reaction, and NO_x formation reaction, which has been verified by a large number of experiments and widely used in the simulation research of hydrocarbon fuels. Because this paper studies the homogeneous compression ignition characteristics of binary mixed fuel under NVO strategies, focusing on the prereaction temperature and component concentration, the original mechanism is simplified and reformed. On the basis of adding hydrogen mechanism, the sensitivity analysis method is used to pick out elementary reactions and substances with high sensitivity to the initial temperature and concentration of the reaction, and, then, the reaction coefficient variation method [31] is used to optimize the parameters of Arrhenius equation which affect the chemical reaction rate.

$$k = AT^b e^{(-E/RT)}, \tag{1}$$

where k is the reaction rate constant, A is the preexponential factor, T is the reaction temperature, b is the temperature exponent, E is the reaction activation energy, and R is the general gas constant. The main optimization objects are A, b, and E. After simplification, the mechanism and thermodynamic data are introduced into the combustion model. The calculation of composition is based on the chemical reaction kinetic process and the definition of fuel physical parameters.

$$\frac{dY_i}{dt} = \frac{\omega_i M_i}{\rho}, \tag{2}$$

where subscript i represents the component of the ith substance, Y is the mass fraction, $\dot{\omega}$ is the chemical reaction rate determined by k, M is the molar mass, and ρ is the ratio of the total mass of the mixture to the system volume. Define the hydrogen volume fraction:

$$\beta_{H_2} = \frac{V_{H_2}}{V_{H_2} + V_{CNG}}. \tag{3}$$

Combined with the physical parameters of the mixed fuel, the molar mass of the mixed fuel at fixed ratio can be calculated as

$$M_F = 16 - 14\beta_{H_2}. \tag{4}$$

The stoichiometric air-fuel ratio of the mixture is

$$l_{0F} = l_{0(H_2)} \frac{2\beta_{H_2}}{M_F} + l_{0(CH_4)} \left(1 - \frac{2\beta_{H_2}}{M_F}\right), \tag{5}$$

where $l_{0(H_2)}$ and $l_{0(CH_4)}$ are the stoichiometric air-fuel ratio of the two fuels, respectively. The aforementioned formulas form the basis for solving the material composition.

2.2. Zero-Dimensional Single-Zone Model. The zero-dimensional single-zone combustion model considers that the temperature, pressure, and components of the in-cylinder charges are uniformly distributed, which accords with the homogeneous premixing conditions of HCCI combustion. The model provides temperature input for the reaction mechanism, thus calculating various combustion process parameters. It is assumed that the mixture is an ideal gas, and the working fluid is in a sealed state without leakage loss. The solution of combustion heat release rate is based on the energy conservation equation of the first law of thermodynamics:

$$\frac{d(me)}{dt} + p\frac{dV}{dt} = \sum \dot{m}_i h_i - \frac{\delta Q_W}{dt}, \tag{6}$$

where subscript i represents the component of the ith substance, e is the specific thermodynamic energy of the working fluid, p is the in-cylinder pressure, V is the working volume of the cylinder, $\dot{m}$ is the mass flow rate of substances in the cylinder, h is specific enthalpy, and Q_W is the heat transfer quantity from working fluid to the cylinder wall, which is determined by the heat transfer model:

$$\frac{\delta Q_W}{dt} = (T - T_W) S_t z, \tag{7}$$

where T_W is the average temperature of cylinder wall, S_t is the effective heat transfer area, and z is the heat transfer coefficient. Coupled with the energy equation, the heat transfer submodel provides boundary conditions for calculating the temperature field, such as cylinder wall temperature, cylinder temperature distribution, and heat flow distribution, which reflects the heat transfer and heat loss of working fluid to the combustion chamber wall. For homogeneous zero-dimensional compression ignition model, z is given by the widely accepted Woschni correlation [19, 32]:

$$z = 0.1298 D^{-0.2} p^{0.8} T^{-0.53} v^{0.8}, \tag{8}$$

where D is the cylinder diameter and v is the characteristic velocity which represents the statistical average motion characteristics of substances in the cylinder:

$$v = C_1 v_m + C_2 \frac{V_s T_j}{p_j V_j} (p - p_{mt}), \tag{9}$$

where v_m is the average speed of piston, V_s is the working volume of cylinder, the parameters with subscript j represent the state of working fluid at any time from the closing time of intake valve to the start of combustion, p_{mt} is the engine drag pressure, C_1 is 0.28, and C_2 is 0 in the compression stroke and 3.34×10^{-3} in the power stroke. Temperature changes during combustion duration are expressed by

$$\frac{dT}{dt} = \frac{1/\rho \sum e_i \omega_i M_i + RT/V_s M_h (dV/dt)}{\sum Y_i (C_v)_i}, \quad (10)$$

where subscript i is the ith substance component, M_h is the average molar mass of mixture, and C_v is the specific heat capacity at constant pressure. This formula and formula (2) can be regarded as a first-order nonlinear system of equations with $i + 1$ unknowns.

2.3. Geometric Model of Engine Cylinder. The variation of cylinder volume with time can be obtained from the geometric relationship:

$$V(t) = V_C + \frac{\pi D^2 L_A}{4}\left(R + 1 - \cos\theta - \sqrt{R^2 - \sin^2\theta}\right), \quad (11)$$

where V_C is the volume of combustion chamber, L_A is crank length, R is the length ratio of connecting rod to crank, and θ is the crank angle. In the simulation, the change rate of scavenging volume is often used.

$$\frac{d(V(t)/V_C)}{dt} = \frac{(\varepsilon - 1)\sin\theta}{2}\left[1 + \frac{\cos\theta}{\sqrt{R^2 - \sin^2\theta}}\right]\frac{d\theta}{dt}, \quad (12)$$

where ε is the compression ratio. By combining the above equations, the combustion model, heat transfer model, and geometric model are comprehensively used in combination with the reaction mechanism and physical property parameter data; then, the parameter values characterizing the combustion dynamic process of the engine at any time in the cylinder could be obtained under the conditions of given initial pressure, temperature, and initial concentration of various material components.

2.4. EGR Rate Calculation under NVO Strategy. In every cycle, combustion dynamic process is affected by the gas change process. The EGR rate is an important parameter connecting the two processes; the conventional method of calculating EGR rate is determined by measuring CO_2 concentration in exhaust pipe after compression stroke and exhaust stroke, which is not suitable for describing the internal EGR effect formed by NVO strategies. According to the combustion reaction equation and the data obtained by simulation, the EGR rate under stoichiometric condition is theoretically derived. It is assumed that the fuel is completely burned, the gas in the cylinder is evenly mixed, and the valve opening and closing are not affected by the response delay of the valve train and the pressure difference between inside and outside the cylinder.

$$\phi_E = \frac{m_r'}{m_r' + m_h}, \quad (13)$$

where m_h is the mass of the mixture charged into the cylinder after the intake valve is closed and m_r' is the mass of residual exhaust gas in the cylinder after the exhaust valve is closed. Obviously, m_r' is determined by the combustion process of the previous cycle and the closing time of the exhaust valve.

$$m_r' = \frac{p_{\mathrm{EVC}} V_{\mathrm{EVC}}}{RT_{\mathrm{EVC}}} \frac{\left(1 + \gamma_{O_2}\right) y + 4}{\left(28 + 8\gamma_{O_2}\right) y + 64\gamma_{O_2} + 112}, \quad (14)$$

where the parameters with subscript EVC indicate the state of in-cylinder working fluid at the closing time of the exhaust valve, γ_{O_2} is the volume fraction of oxygen in the air, and y is defined as the molar ratio of hydrogen atoms to carbon atoms in the mixed fuel, which has a certain correlation with β_{H_2}. m_r' and the subsequent intake process jointly affect the value of m_h.

$$m_h = \left(\frac{p_{\mathrm{IVC}} T_{\mathrm{IVC}}}{RT_{\mathrm{IVC}}} - \frac{p_{\mathrm{EVC}} T_{\mathrm{EVC}}}{RT_{\mathrm{EVC}}}\right)\left[\frac{M_A(1 + l_{0F}) M_F}{M_A + l_{0F} M_F}\right], \quad (15)$$

where the parameters with subscript IVC indicate the state of in-cylinder working fluid at the closing time of intake valve and M_A is the molar mass value of air. Other parameters of this formula are given by formula (4) and formula (5).

3. Test Validation

In order to validate the accuracy of the simulation model, a bench test was carried out on a natural gas-hydrogen-fueled engine modified from a four-stroke naturally aspirated water-cooled diesel engine. The main technical parameters of the engine are listed in Table 1. The schematic diagram of the test bench is shown in Figure 1. Hydrogen and natural gas stored in high-pressure gas cylinders, respectively, flow into the Venturi mixer through the pressure reducing valve, then mix with air to enter the cylinder in the way of intake port injection. The experiment was conducted at 1100 rpm, the equivalent ratio is 0.4, and the hydrogen volume fraction is 5%. The detailed introduction and test accuracy of various instruments used have been given in previous studies [33].The initial temperature, pressure, and other data of the model are measured from the test, and the simulation conditions are consistent with the test conditions.

The comparison between the experimental and simulated values of pressure, temperature, and heat release rate is shown in Figures 2–4. Through comparison, it can be seen that the agreement between the calculation result and the experimental data is reasonable for all the three indicators. It also can be found that the peak values of simulated pressure and temperature are slightly higher than the experimental values, the ignition phase is slightly later, and the rising rate of pressure and temperature at the initial combustion period and the falling rate at the end combustion period are also faster. This is because the heat transfer loss considered by the simulated combustion model is less than the real situation. The mixing degree of working fluid is higher, and the combustion process is close to constant volume heat release. In the experiment, due to the influence of turbulence in cylinder, the rise of temperature and pressure is uneven; in some areas, better ignition conditions can be formed to accelerate spontaneous combustion. The fluctuant rising process

Table 1: Main parameters of test engine.

Parameter	Value
Displacement (L)	0.815
Bore × stroke (mm)	95 × 115
Compression ratio	17 : 1
Rod length × crank radius (mm)	210 × 57.5
Calibration power/speed (kW/rpm)	10.6/2200
Calibration fuel consumption rate (g/kWh)	≤244.8
Maximum torque/speed (Nm/rpm)	50.2/1760
Exhaust valve opening timing (°CA BBDC)	43
Intake valve opening timing (°CA BTDC)	15
Exhaust valve closing timing (°CA ATDC)	15
Intake valve closing timing (°CA ABDC)	33

makes the local pressure and temperature appear too high or too low, and the incomplete uniformity of mixture also prolongs the after-combustion period. The maximum error of the pressure between simulation value and the test value is 4.92%, while the maximum temperature error between the simulation value and the test value is 4.68%. In the whole crank angle range of the power process, the simulated data possess good order of magnitude and accuracy, which indicates that the simulation model can reliably reflect the real performance of the engine.

4. Results and Discussion

4.1. Influence of Changing the Closing Time of Exhaust Valve on Combustion Emissions. Figures 5–11 show the influence of changing the timing of closing the exhaust valve (EVC) on the combustion and emission characteristics of the engine while keeping the opening of the exhaust valve (EVO), opening of the intake valve (IVO), closing of the intake valve (IVC), and the valve lift unchanged. A set of valve lift curves are obtained every 15°CA ahead of TDC in the gas exchange process. The initial simulation conditions are equivalent ratio of 1, engine speed of 1000 rpm, intake temperature of 400 K, intake pressure of 0.1 MPa, hydrogen volume fraction of 5%, and fuel mass flow rate of 6.5 g/s. Because IVO is kept at 15° before TDC, the negative overlap angle formed under the current strategy is 0-75°.

It can be seen from Figure 5 that with the advance of EVC time, the EGR rate increases. This is because the sooner the exhaust valve is closed, the less exhaust gas is discharged from the exhaust pipe and the more exhaust gas is intercepted in the cylinder. The EGR rate increased by 19.47 percentage points from 15° to 90°. Figure 6 displays that the charging efficiency decreases with increases in the advancement of EVC, which is due to the fact that although IVO remains unchanged, the more exhaust gas remains in the cylinder because of the advanced EVC, and the pressure difference between the cylinder and the throat of the intake valve when the intake valve is opened is smaller compared with the original engine without EGR, hence hindering the charging of fresh mixture. At the same time, the heating of the new air by the exhaust gas will cause decreases in the air density in the intake state, and the amount of gas actually entering the cylinder decreases slightly. In addition, because the piston is still in the upstroke stage at IVO, for the naturally aspirated engine, there may be a certain degree of backfire in the cylinder, and the earlier the EVC, the more serious the backfire phenomenon will be, which will further reduce the amount of fresh air filled in the cylinder. When the exhaust valve closes from 15° to 90° in advance, the charging efficiency decreases by 26.15%.

It can be seen from Figures 7 and 8 that with the advance of EVC, the combustion pressure and temperature decrease. This is because the EGR rate increases with the advance of EVC, and the dilution degree of new gas by the increased exhaust gas also increases, thus increasing the engine output power loss. From 15° to 90°, the maximum pressure and temperature decreased by 18.2% and 17.4%, indicating that the advance degree of EVC has great influence on them. The time of reaching the highest pressure and temperature is slightly earlier, which indicates that the improvement of combustion process increases when the exhaust valve is closed in advance.

It can be seen from Figures 9 and 10 that with the advance of EVC time, the maximum value of the pressure rise rate and the heat release rate decreases gradually. The main reasons for this change are as follows: the earlier EVC is, the larger NVO angle is, the more exhaust gas remains, and the higher EGR rate is. Because the exhaust gas with higher specific heat capacity and lower oxygen content has both dilution and cooling effect, the maximum temperature in the cylinder decreases, thus slowing down the rate of combustion reaction in the cylinder, reducing the pressure rise rate, and making the combustion more stable, which is helpful to weaken the rough working phenomenon (a common characteristic in general HCCI engines) and reduce the knocking tendency, the thermal load of working components, the vibration, and noise of whole machine.

Figure 11 shows that with the advance of EVC time, NO_x emission decreases relatively. From the foregoing analysis, it can be seen that the dilution of exhaust gas reduces the charge efficiency and the oxygen concentration of the mixture; in addition, the exhaust gas slows down the heat release rate of and lowers the maximum temperature. According to the formation mechanism of NO_x, oxygen enrichment and high temperature are favorable conditions; hence, NO_x emission decreases. In the later stage, the temperature decreases with the downstroke movement of piston, so the total amount of NO_x formation no longer rises and tends to be stable.

4.2. Influence of Changing Opening Time of Intake Valve on Combustion Emission. Figures 12–18 show the influence of changing IVO time on engine combustion and emission while keeping EVO, EVC, IVC, and valve lift unchanged. A set of valve lift curves are obtained every 15°CA after the intake valve is delayed from the top dead center in the gas exchange process, and the simulated initial conditions remain unchanged. Because EVC is kept at 15° after TDC, the NVO angle that can be formed under the current strategy is 0-75°, but its negative overlapping area is after TDC, while

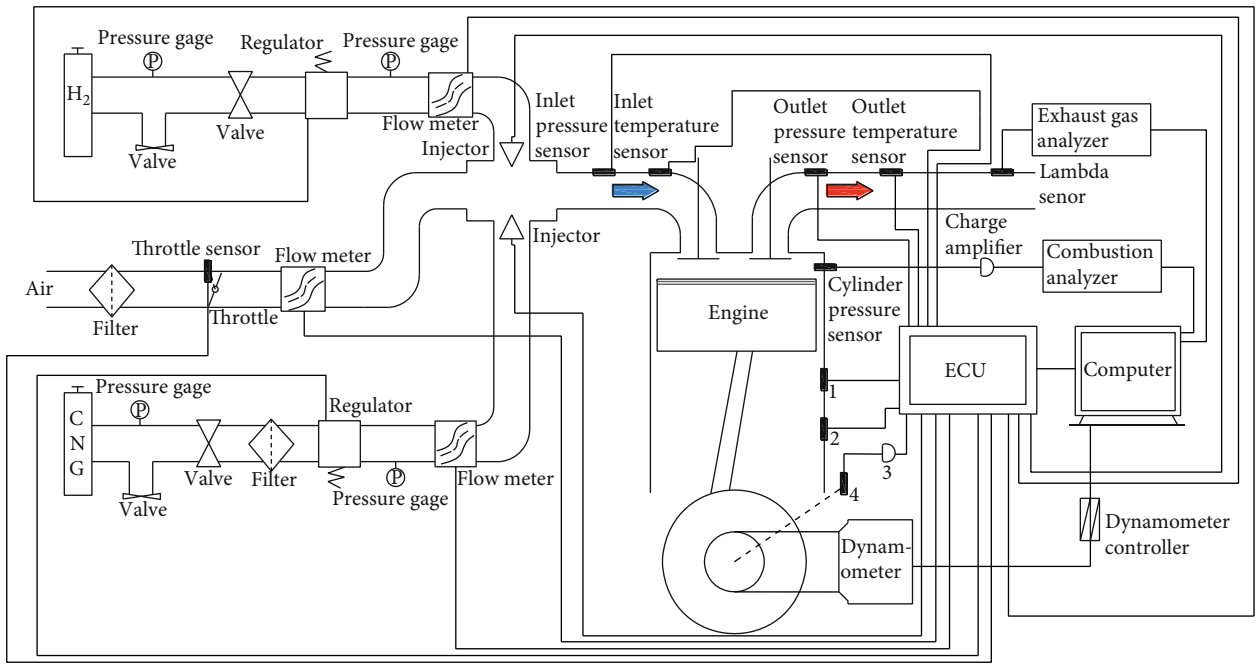

(1) coolant water temperature sensor
(2) lubricating oil temperature sensor
(3) charge amplifier
(4) crankshaft sensor

Figure 1: The schematic diagram of the test bench.

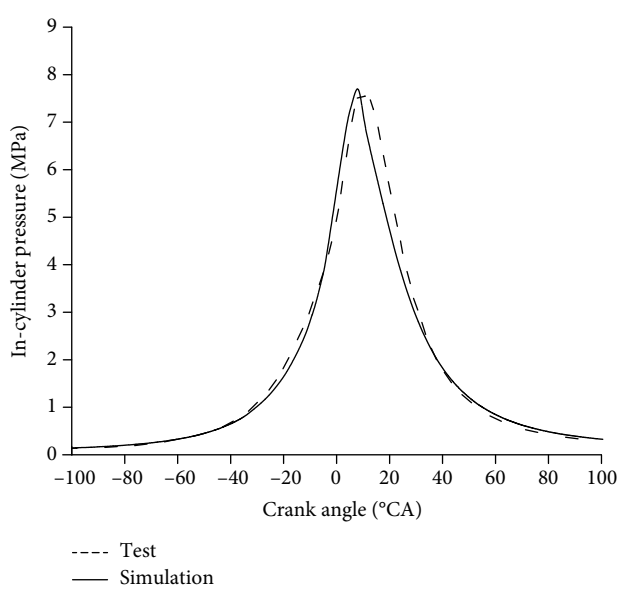

Figure 2: Comparison between simulated and measured pressure.

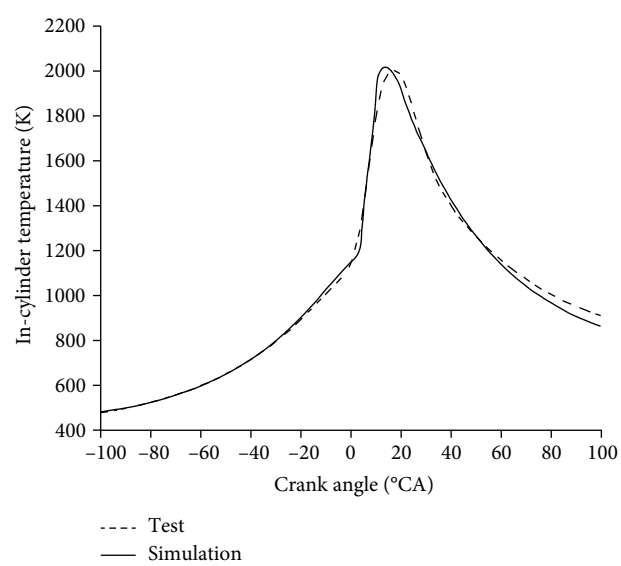

Figure 3: Comparison between simulated and measured temperature.

the area of the scheme in Section 4.1 is before TDC. It can be seen from Figures 12 and 13 that the EGR rate increases with the delay of IVO, and the charging efficiency shows a downward trend accordingly. This is because the later the intake valve open, the less fresh air is started into the cylinder. Although the residual exhaust gas in the cylinder keeps a fixed amount due to the fixed EVC timing, the fresh air quantity is affected by the descending degree of piston. The later the intake valve opens, the shorter the actual intake duration. From 15° to 90°, the intake valve delayed opening, the EGR rate increased by 10.06 percentage points, and the charging efficiency decreased by 17.51%. On the whole, when IVO is changed, the enhancement of EGR rate and the weakening of charging efficiency are slightly smaller than those when

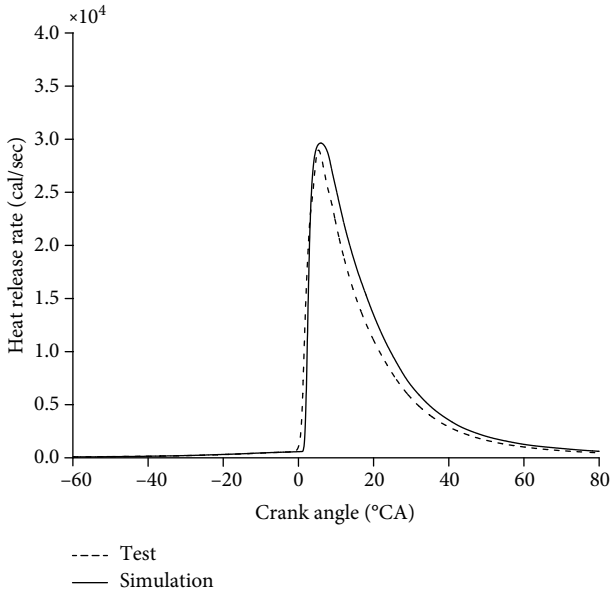

Figure 4: Comparison between simulated and measured heat release rate.

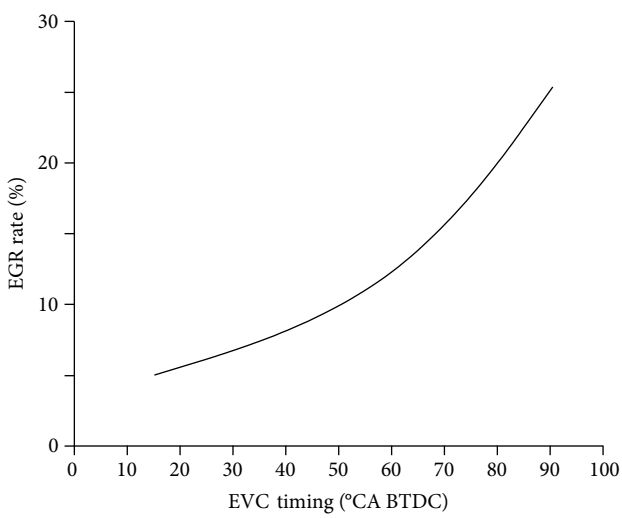

Figure 5: Influence of advanced degree of EVC timing on EGR rate.

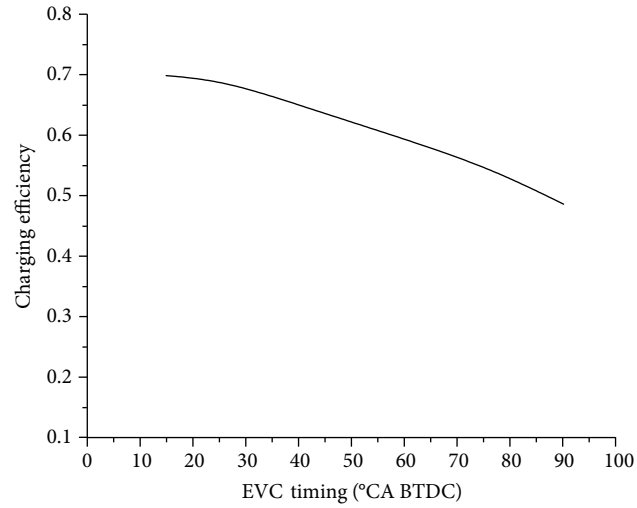

Figure 6: Influence of advanced degree of EVC timing on charging efficiency.

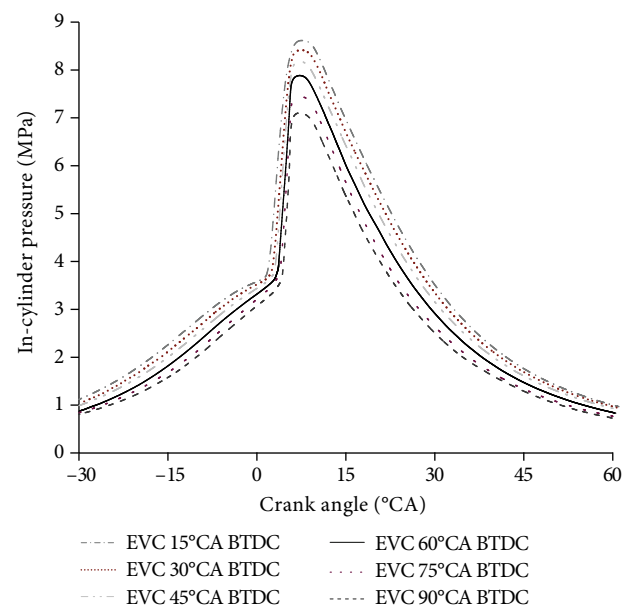

Figure 7: Influence of advanced EVC on pressure.

EVC is changed individually. This shows that although the residual exhaust gas under the current scheme is limited, the fresh gas also decreases, and the overall relative concentration of old and new gas is similar under the two schemes.

It can be seen from Figures 14 and 15 that the peak values of in-cylinder pressure and temperature gradually decrease, and the phase of reaching the peak value is slightly advanced in the delayed IVO. From 15° to 90°, the peak pressure in the cylinder decreased by 9.2% and the maximum temperature decreased by 9.7%. Compared with the EVC scheme, in the same NVO angle, when IVO is changed individually, the peak value of pressure and temperature decreases little. This is because the fixed EVC timing makes the amount of exhaust gas intercepted in the cylinder keep constant, the increment of exhaust gas proportion is relatively smaller, and the power loss is less.

It can also be seen that when IVO is changed, the ignition time of fuel also changes, and this effect can be analyzed with reference to Figures 16 and 17. With the delay of IVO timing, the pressure rise rate and combustion heat release rate gradually decrease, but the ignition phase is advanced; this is because the decrease of fresh air amount caused by the delayed closing of intake valve; under the same residual exhaust gas amount, the average heating degree to fresh air is instead enhanced, and Figure 15 also reveals that the temperature at the starting point of combustion increases in delay of intake valve opening, which is beneficial to the progress of HCCI. In the scheme of changing EVC, the heating

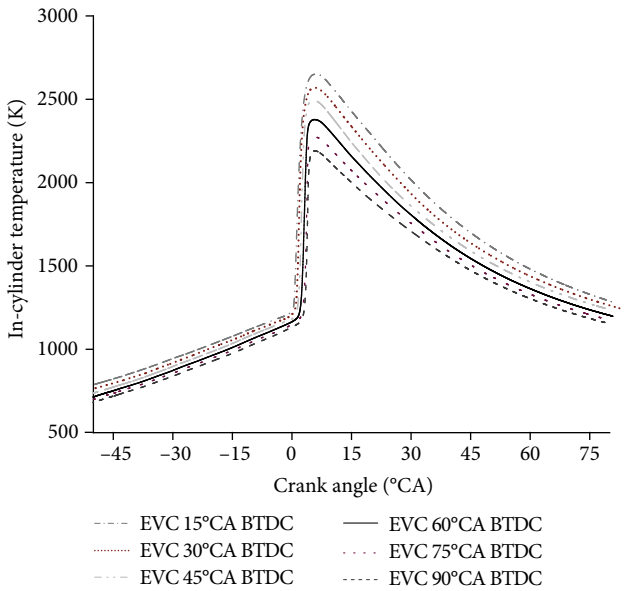

Figure 8: Influence of advanced EVC on temperature.

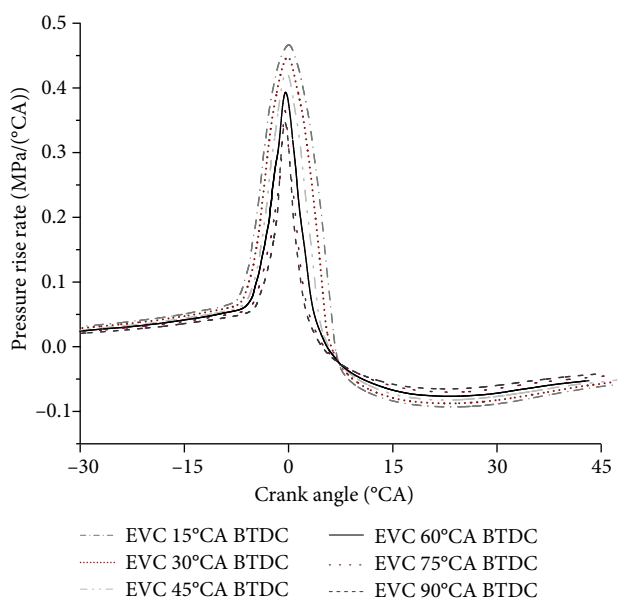

Figure 9: Influence of advanced EVC on pressure rise rate.

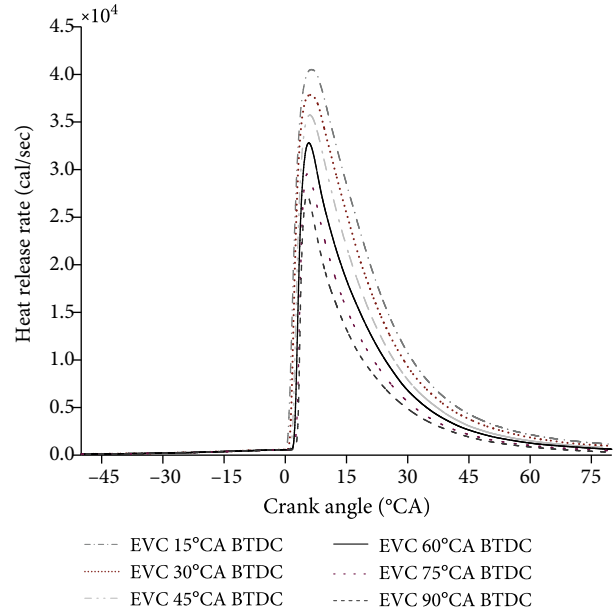

Figure 10: Influence of advanced EVC on heat release rate.

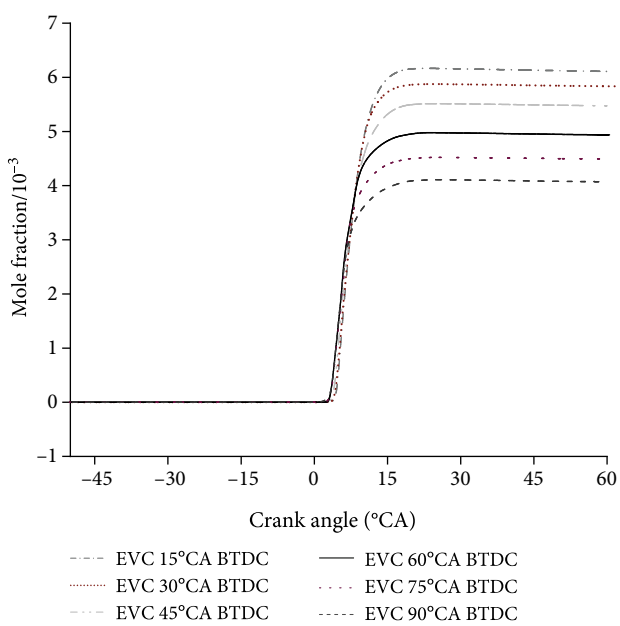

Figure 11: Influence of advanced EVC on NO_x emission.

contribution of exhaust gas is only reflected in the advance of the phase corresponding to the peak value of combustion pressure and combustion temperature; hence, the influence of changing IVO strategy is mainly reflected in the change of combustion starting point, and it can be further judged that the main influencing factor of combustion starting point is fresh air quantity rather than EGR rate, because when changing EVC individually, the IVO remains unchanged but opens earlier than TDC, and the fresh air quantity is generally higher than that of changing IVO strategy individually; although the amount of exhaust gas remains large, the average degree of heating new gas is insufficient. However, when IVO is changed individually, although the amount of exhaust gas decreases due to the original engine exhaust valve phase, the amount of fresh gas also decreases, which makes it easier to be heated by the limited amount of exhaust gas, and the effect of early ignition is more obvious. The above comparison shows that although the heating effect of intake air is affected by EGR rate, it is more sensitive to the amount of fresh air. It can be seen from the change of EGR rate that although the range of EGR rate can be achieved by changing EVC individually is larger than that by changing IVO

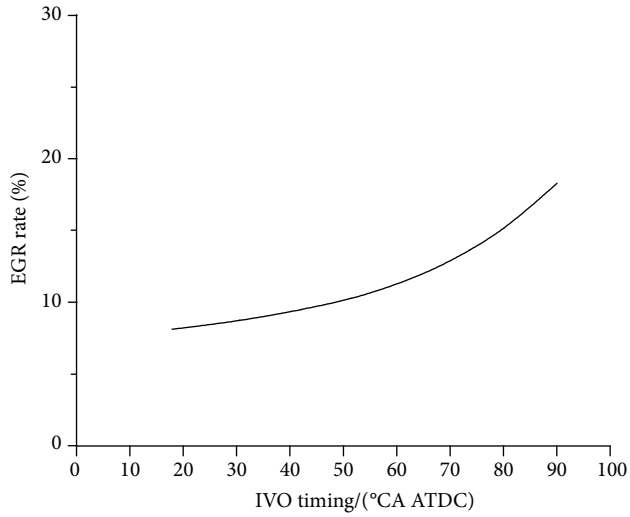

Figure 12: Influence of delayed degree of IVO on EGR rate.

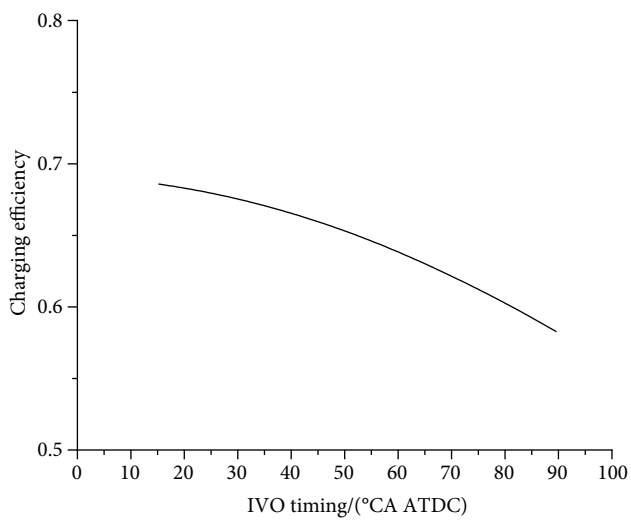

Figure 13: Influence of delayed degree of IVO on charging efficiency.

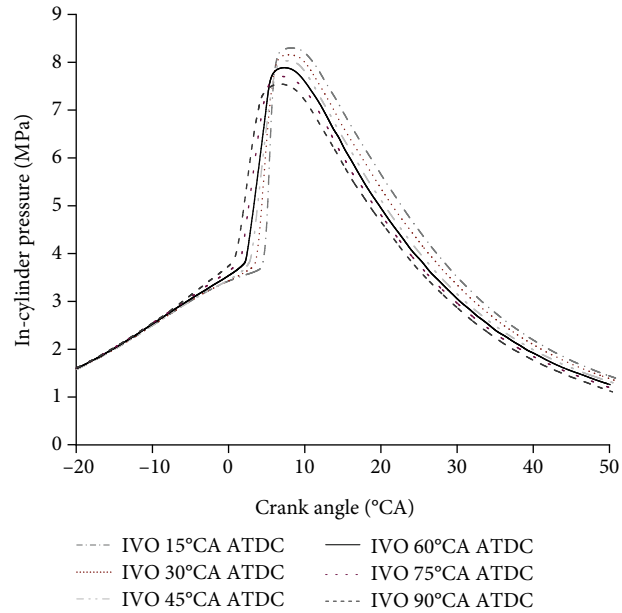

Figure 14: Influence of delayed IVO on pressure.

individually, the increase of fresh air makes it more difficult to heat exhaust gas even under the condition of similar exhaust gas ratio.

Figure 18 displays that NO_x emission decreases with the delay of IVO timing. This is because the dilution of exhaust gas reduces the oxygen concentration in the cylinder, and at the same time, the exhaust gas slows down the heat release rate, reduces the maximum temperature of combustion, and inhibits the oxygen-enriched high temperature condition. Compared with changing EVC time individually, because the exhaust valve maintains the original engine phase, the amount of exhaust gas is not much, and the increase of EGR rate, the reduction of temperature, pressure, and heat release rate are not much, so the NO_x emission is not much improved.

4.3. Influence of Changing the Opening and Closing Time of Intake and Exhaust Valves on Combustion Emissions. If the advance angle of EVC is increased to a certain degree, the effect of ignition time advanced by EGR is not obvious, which may lead to the failure of HCCI, while when IVO is delayed, the EGR rate does not change much, and the decrease of combustion temperature and improvement of NOx are not obvious. For improving the ignition and achieving a better EGR rate, consider combining the two schemes, which means changing the IVO and EVC simultaneously. Figures 19–25 show the effects of changing EVC and IVO on engine combustion and emission characteristics while keeping EVO, IVC, and valve lift unchanged. The intake valve is delayed in opening while exhaust valve is earlier in closing. Other initial conditions are unchanged, and the NVO angle that can be formed under the current strategy is 30°-180°. Because the interval value of angle that changed is symmetrical about TDC, this strategy is also called symmetric NVO strategy.

Figures 19 and 20 display that the EGR rate increases by 47.92 percentage points, and the charging efficiency decreases by 50.77%. It can be seen that the symmetric NVO strategy can produce a larger EGR rate, because the earlier the exhaust valve closes, the more exhaust gas be intercepted, while the later the intake valve opens, the less fresh mixed gas could be, and the loss of charging efficiency will be larger than that when EVC or IVO is changed individually. In addition, when the EVC is changed individually, the pressure difference between inside and outside the cylinder caused by the exhaust gas intercepted by the early closing of the exhaust valve, which leads to the backfire phenomenon, can be effectively avoided under this scheme because the intake air is delayed to open and the piston is in downstroke. Compared with the IVO strategy, the average heating effects on limited fresh air are also better because the exhaust valve is closed earlier.

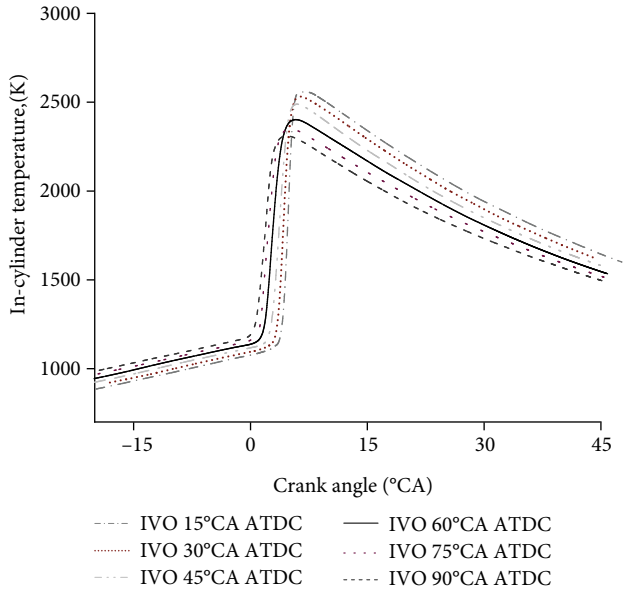

Figure 15: Influence of delayed IVO on temperature.

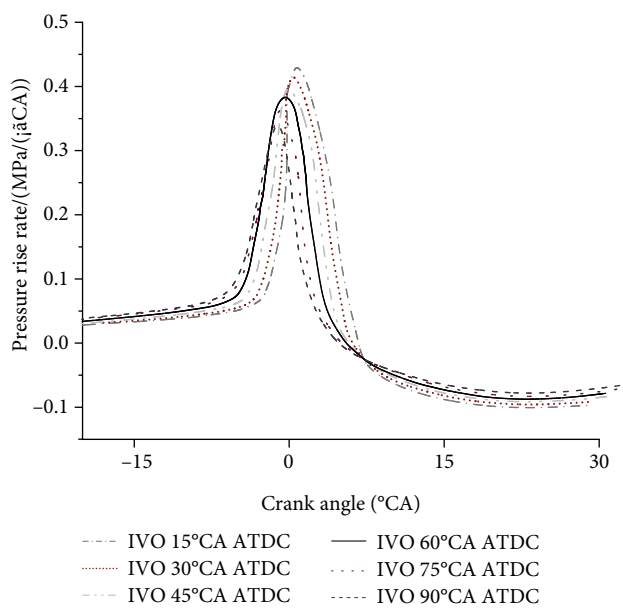

Figure 16: Influence of delayed IVO on pressure rise rate.

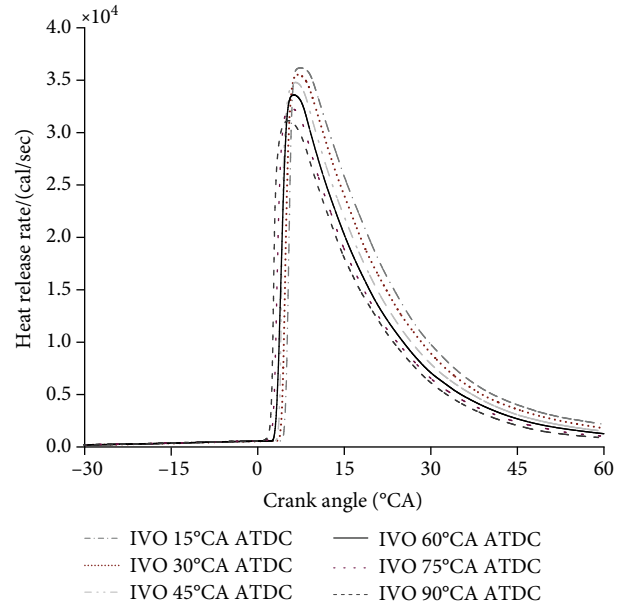

Figure 17: Influence of delayed IVO on heat release rate.

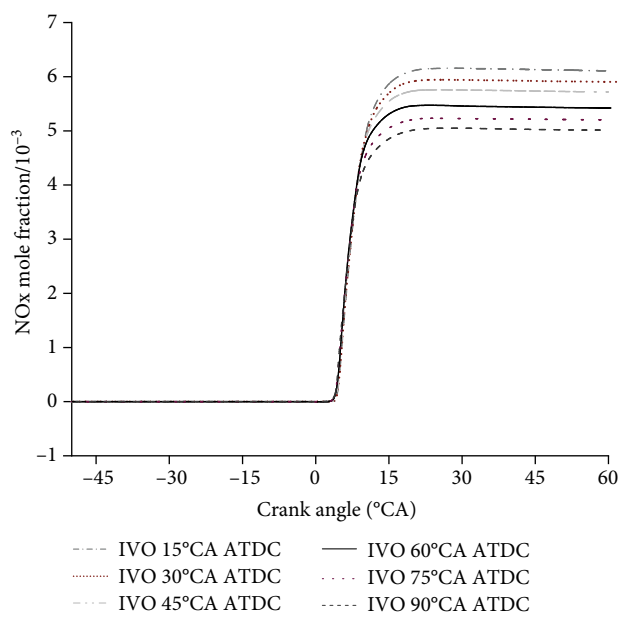

Figure 18: Influence of delayed IVO on NO_x emission.

With the increase of symmetric NVO angle, the maximum pressure and temperature decreased by 29.2% and 20.7%, respectively. The decrease is greater than that of IVO or EVC individual change. The pressure rise rate and heat release rate decrease obviously with the increase of symmetric NVO angle. Because the heat release rate is mainly affected by the change of EGR rate, and the range of EGR rate formed by symmetric NVO is larger, the combustion reaction is also eased greatly, and the slowed heat release also causes the pressure rise rate to decrease, which is beneficial to reduce the engine speed and torque variation, prevent the possibility of knocking, and make the engine work more smoothly. Changing intake and exhaust valve timing simultaneously has a significant impact on fuel ignition timing. The greater the NVO angle, the greater the fuel ignition advance, and the temperature before ignition is correspondingly enhanced by exhaust heating. This is because with the increase of NVO angle, the amount of exhaust gas in the cylinder increases while the amount of fresh air decreases. The heating effect of exhaust gas on fresh air is better than that of individually changing IVO strategy with fixed exhaust gas amount at the same intake delayed opening degree and also better than that of individually changing EVC strategy with more fresh air amount at the same exhaust advanced

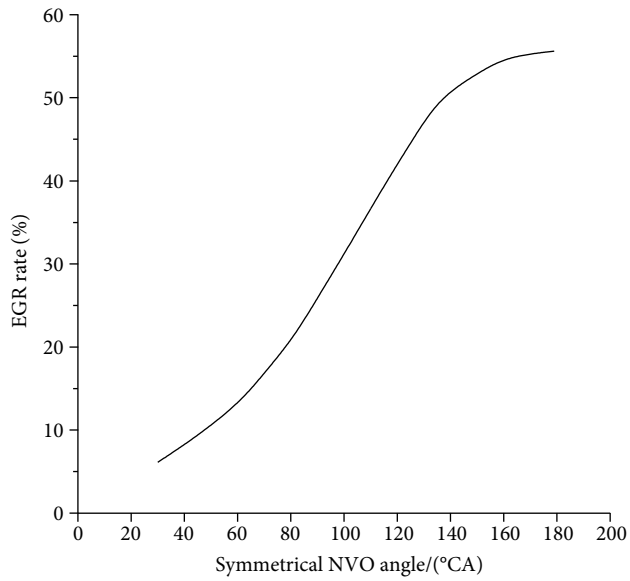

Figure 19: Influence of symmetric NVO on EGR rate.

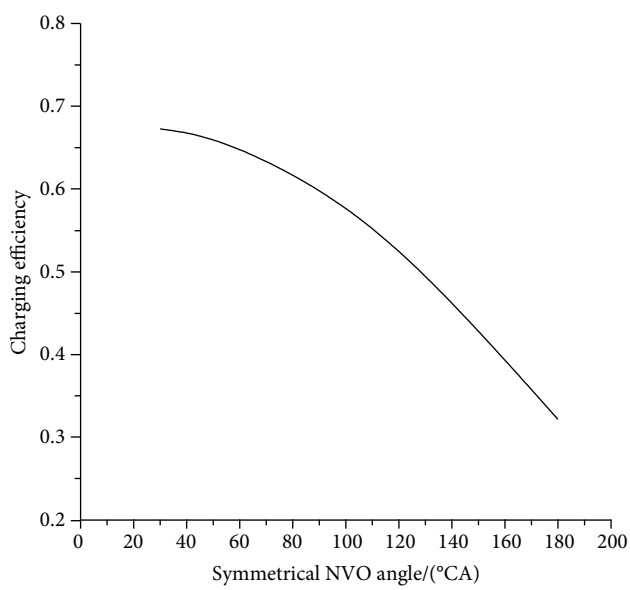

Figure 20: Influence of symmetric NVO on charging efficiency.

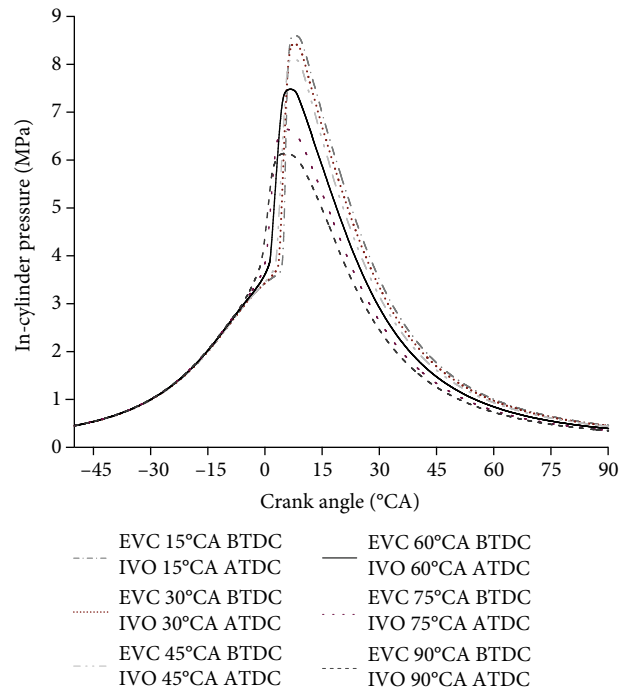

Figure 21: Influence of symmetric NVO on pressure.

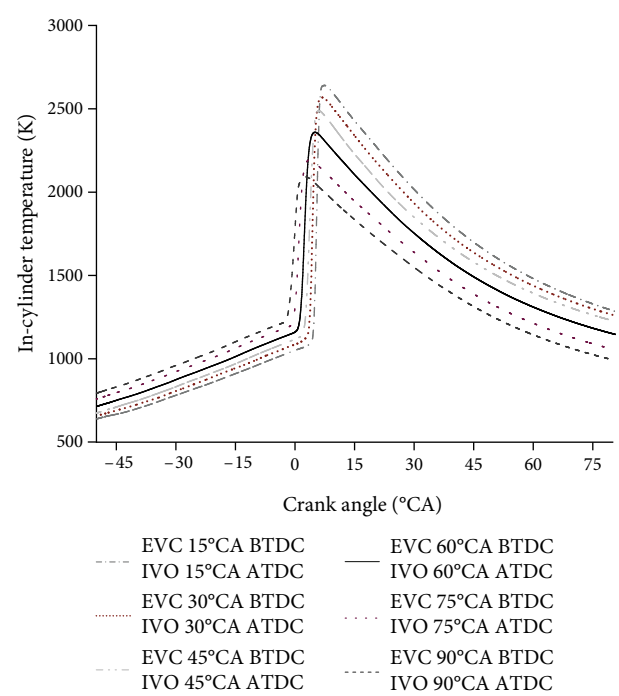

Figure 22: Effect of symmetric NVO on temperature.

closing degree. However, when the NVO angle is too large, for example, when the angle of advanced EVC and delayed IVO is greater than 75°, the mixed fuel is excessively advanced to release heat before the top dead center, which makes the power process bears a part of the compression negative work loss and reduces the constant volume heating degree, so it should be avoided.

Figure 25 displays the influence of symmetric NVO on NO_x emission. It can be seen that with the advance of EVC and the delay of IVO, the NO_x production decreases significantly. From the above analysis, the most important factor affecting NO_x is the maximum temperature, because the symmetric NVO strategy can achieve a larger EGR rate, and the maximum decreases more greatly. The reduction of combustion speed also makes the NO_x production rate slower, which eventually leads to a sharp reduction in the NO_x production.

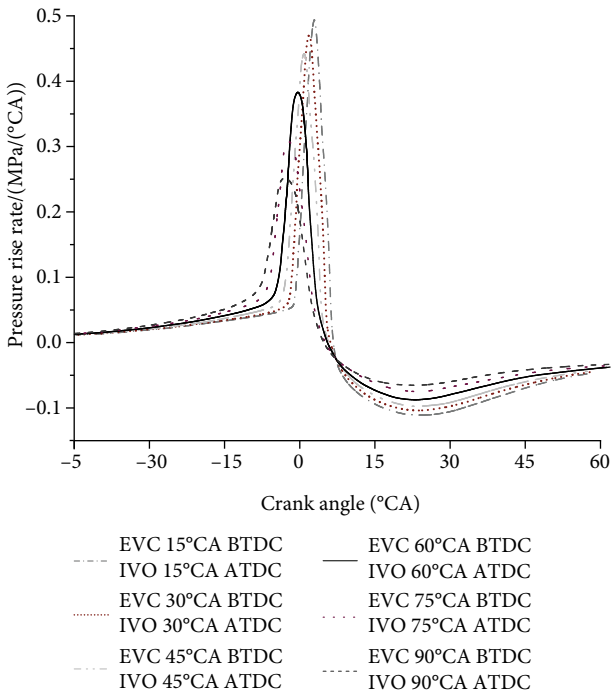

Figure 23: Influence of symmetric NVO on pressure rise rate.

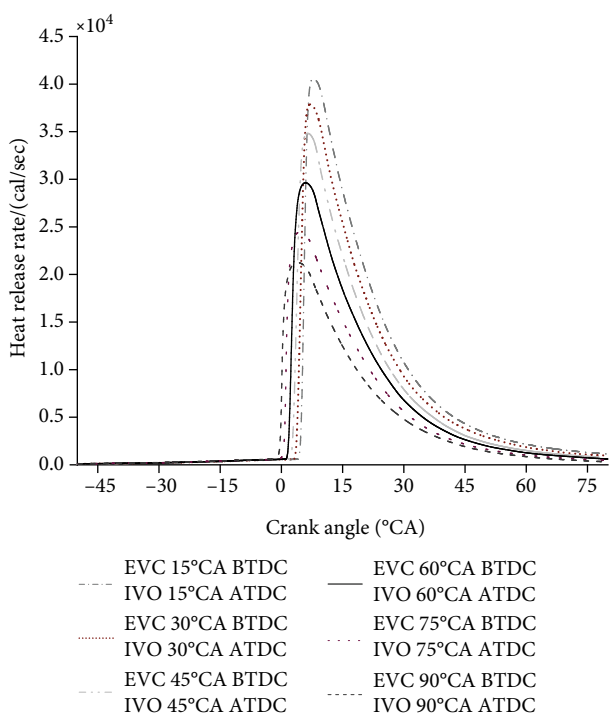

Figure 24: Effect of symmetric NVO on heat release rate.

5. Conclusions

With the development in the energy crisis [34–38] and environmental problems [39–47], the effective control of energy saving and the reduction of emissions in engines are primary areas of focus for scholars. In this study, based on bench test, a simulation for an HCCI engine fueled with natural gas and hydrogen is carried out, and the effect of changing valve timing to form negative valve overlap on in-cylinder combustion process and emission characteristics is investigated.

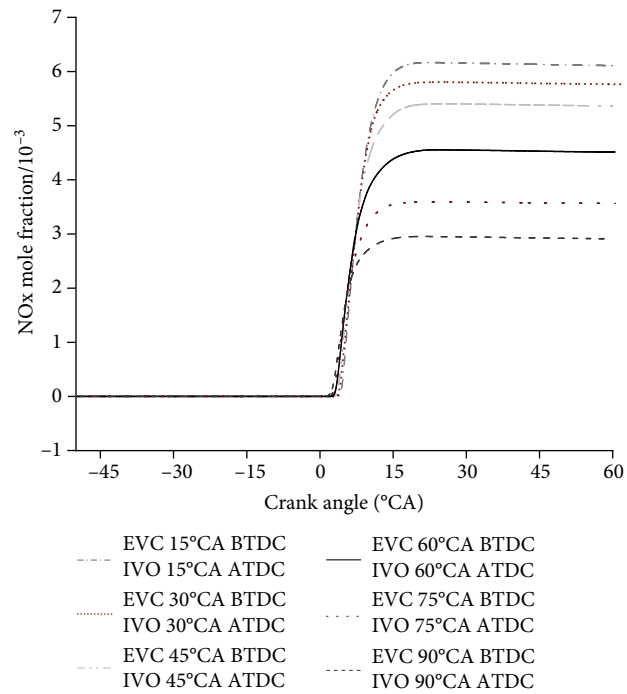

Figure 25: Effect of symmetric NVO on NO_x emission.

The power process of HCCI engine will suffer losses due to the influence of negative valve overlap, more specifically, the amount of residual exhaust gas and EGR rate increase with the increase of negative overlap angle. The maximum decrease of pressure is 18.2% when changing EVC timing individually and 29.2% when changing EVC and IVO simultaneously. The variation range of EGR rate and charging efficiency is small when IVO is changed individually; hence, the power loss is the smallest, with the maximum in-cylinder pressure decrease of only 9.2%.

When the time of EVC or IVO is changed individually, the NVO angle can be formed is the same, but the influence on the heat release starting point is different. Only changing IVO could make the earlier ignition time than changing EVC individually, and the heat release starting point is mainly affected by the average heating influence of working fluid rather than the range of EGR rate, which means it is more sensitive to the fresh air. With more residual exhaust gas and better heating effect, symmetric NVO strategy can significantly affect the ignition time. However, when the NVO angle exceeds 150°, the ignition time is excessively advanced before the top dead center, which is harmful to the heat release process.

Symmetric NVO strategy can achieve the highest EGR rate and has the greatest effect on easing the combustion heat release rate and reducing the pressure rise rate, which is helpful to improve the rough running of HCCI engine, preventing the occurrence of knocking, and enable a wider load

range and a softer combustion heat release process for the HCCI mode of HCNG fuel.

The maximum temperature is the main factor affecting NO_x emission, the maximum decrease of which is 17.4%, 9.7%, and 20.7%, respectively, in the three strategies. The NVO strategy can achieve the greatest emission reduction, while the strategy of changing IVO individually has the minimal effect on the reduction of temperature and heat release rate; hence, the NO_x reduction achieved is also the minimum.

Data Availability

The data used to support the findings of this study are included within the article.

Conflicts of Interest

The authors declare that they have no conflicts of interest regarding the publication of this paper.

Acknowledgments

This work was supported by the National Natural Science Foundation of China (grant no. 51176014) and the Natural Science Foundation of Hunan Province, China (grant no. 2020JJ4616).

References

[1] S.-J. Luo, F.-H. Ma, R. K. Mehra, and Z.-H. Huang, "Deep insights of HCNG engine research in China," *Fuel*, vol. 263, article 116612, 2020.

[2] R. K. Mehra, H. Duan, R. Juknelevičius, and F.-H. Ma, "Progress in hydrogen enriched compressed natural gas (HCNG) internal combustion engines - a comprehensive review," *Renewable & Sustainable Energy Reviews*, vol. 80, pp. 1458–1498, 2017.

[3] R. K. Mehra, H. Duan, S.-J. Luo, A. Rao, and F.-H. Ma, "Experimental and artificial neural network (ANN) study of hydrogen enriched compressed natural gas (HCNG) engine under various ignition timings and excess air ratios," *Applied Energy*, vol. 228, pp. 736–754, 2018.

[4] S. Verhelst and T. Wallner, "Hydrogen-fueled internal combustion engines," *Progress in Energy & Combustion Science*, vol. 35, pp. 490–527, 2009.

[5] H. Chen, J.-J. He, and X.-L. Zhong, "Engine combustion and emission fuelled with natural gas: a review," *Journal of the Energy Institute*, vol. 92, pp. 1123–1136, 2019.

[6] B. Huang, E. Hu, Z. Huang, J. Zheng, B. Liu, and D. Jiang, "Cycle-by-cycle variations of a spark ignition engine fueled with natural gas-hydrogen blends combined with EGR," *Transactions of CSICE*, vol. 29, no. 1, pp. 16–22, 2011.

[7] S. Verhelst, "Recent progress in the use of hydrogen as a fuel for internal combustion engines," *International Journal of Hydrogen Energy*, vol. 39, pp. 1071–1085, 2014.

[8] X.-W. Xiong, F.-H. Ma, and Y. Huang, "Experimental research and mean value modeling of a 20% HCNG engine," *Chinese Internal Combustion Engine Engineering*, vol. 38, no. 4, pp. 134–138, 2017.

[9] M. Fanhua, J. Long, and D. Shangfen, "Experimental study on cycle-by-cycle variations in lean-burn natural gas engine with hydrogen enrichment," *Journal of Mechanical Engineering*, vol. 46, no. 6, pp. 21–26, 2010.

[10] G. Wu, W. Deng, Y.-L. Li, and M. Lei, "Effect of acetone-n-butanol-ethanol (ABE) as an oxygenate on combustion, performance, and emission characteristics of a spark ignition engine," *Journal of Chemistry*, vol. 2020, Article ID 7468651, 11 pages, 2020.

[11] Y. Wang, F.-H. Ma, H.-Q. Liu, and Y. Li, "Influence factors of the lean operation limit for a spark ignition hydrogen enriched natural gas engine," *Transactions of the Chinese Society for Agricultural Machinery*, vol. 39, no. 7, pp. 9–13, 2008.

[12] D. Hao, R. K. Mehra, S. Luo, Z. Nie, X. Ren, and M. Fanhua, "Experimental study of hydrogen enriched compressed natural gas (HCNG) engine and application of support vector machine (SVM) on prediction of engine performance at specific condition," *International Journal of Hydrogen Energy*, vol. 45, pp. 5309–5325, 2020.

[13] J. Zhao, F. Ma, X. Xiong et al., "Effects of compression ratio on the combustion and emission of a hydrogen enriched natural gas engine under different excess air ratio," *Energy*, vol. 59, pp. 658–665, 2013.

[14] D. Yap, A. Megaritis, S. Peucheret, M. L. Wyszynski, and H. M. Xu, "Effect of hydrogen addition on natural gas HCCI combustion," *SAE Technical Paper*, 2004.

[15] W. Yong and J. Park, "Parametric study on combustion characteristics of virtual HCCI engine fueled with methane-hydrogen blends under low load conditions," *International Journal of Hydrogen Energy*, vol. 44, pp. 15511–15522, 2019.

[16] H. Song and S. Song, "Predicting performance of a methane-fueled HCCI engine with hydrogen addition considering knock resistance," *International Journal of Hydrogen Energy*, vol. 40, pp. 15749–15759, 2015.

[17] A. Yousefi, A. Gharehghani, and M. Birouk, "Comparison study on combustion characteristics and emissions of a homogeneous charge compression ignition (HCCI) engine with and without pre-combustion chamber," *Energy Conversion and Management*, vol. 100, pp. 232–241, 2015.

[18] E. Neshat and R. K. Saray, "Development of a new multi zone model for prediction of HCCI (homogenous charge compression ignition) engine combustion, performance and emission characteristics," *Energy*, vol. 73, pp. 325–339, 2014.

[19] N. P. Komninos and C. D. Rakopoulos, "Heat transfer in hcci phenomenological simulation models: a review," *Applied Energy*, vol. 181, pp. 179–209, 2016.

[20] M.-Z. Pan, W.-W. Qian, H.-Q. Wei, D.-Q. Feng, and J.-Y. Pan, "Effects on performance and emissions of gasoline compression ignition engine over a wide range of internal exhaust gas recirculation rates under lean conditions," *Fuel*, vol. 265, article 116881, 2020.

[21] H. A. El-Din, M. Elkelawy, H. Panchal, and K. K. Sadasivuni, "Optimization of the multi-carburant dose as an energy source for the application of the HCCI engine," *Fuel*, vol. 253, pp. 15–24, 2019.

[22] H.-F. Liu, M.-F. Yao, B. Zhang, and Z.-Q. Zheng, "Effects of inlet pressure and octane numbers on combustion and emissions of a homogeneous charge compression ignition (HCCI) engine," *Energy & Fuels*, vol. 22, no. 4, pp. 2207–2215, 2008.

[23] H.-F. Liu, M.-F. Yao, B. Zhang, and Z.-Q. Zheng, "Influence of fuel and operating conditions on combustion characteristics of a homogeneous charge compression ignition engine," *Energy & Fuels*, vol. 23, no. 3, pp. 1422–1430, 2009.

[24] Z.-Y. Zhang, G.-Y. Dong, J. Deng, and L.-G. Li, "A numerical study on the effects of internal EGR on HCCI combustion and free ion formation," *Automotive Engineering*, vol. 31, no. 10, pp. 905–910, 2009.

[25] M. Elkelawy, Y.-S. Zhang, H. A. El-Din, and J.-Z. Yu, "A comprehensive modeling study of natural gas (HCCI) engine combustion enhancement by using hydrogen addition," *SAE Technical Paper*, 2008.

[26] O. Lang, W. Salber, and J. Hahn, "Thermodynamical and mechanical approach towards a variable valve train for the controlled auto ignition combustion process," *SAE Paper*, 2005.

[27] K. Poorghasemi, R. K. Saray, K. Bahlouli, and A. Zehni, "3D CFD simulation of a natural gas fueled HCCI engine with employing a reduced mechanism," *Fuel*, vol. 182, pp. 816–830, 2016.

[28] H. Liu, Z. Zheng, M. Yao et al., "Influence of temperature and mixture stratification on HCCI combustion using chemiluminescence images and CFD analysis," *Applied Thermal Engineering*, vol. 33-34, pp. 135–143, 2012.

[29] P. L. Perez and A. L. Boehman, "Effects of the chemical structure and composition of surrogate gasoline fuels on homogeneous charge compression ignition combustion in a single-cylinder engine," *Energy & Fuels*, vol. 28, no. 5, pp. 3377–3390, 2014.

[30] G. P. Smith, D. M. Golden, M. Frenklach et al., *GRI-3.0 Detailed Mechanism*, Berkeley, 2004, http://www.me.berkeley.edu/gri_mech/.

[31] Y. Ra and R. A. Reitz, "A reduced chemical kinetic model for IC engine combustion simulations with primary reference fuels," *Combustion & Flame*, vol. 155, no. 4, pp. 713–738, 2008.

[32] G. A. Woschni, "Universally applicable equation for the instantaneous heat transfer coefficient in the internal combustion engine," *SAE Paper*, 1967.

[33] Y.-L. Li and J.-C. Shen, "Numerical simulation of combustion characteristics for a HCCI engine fueled with natural gas and hydrogen," *Chinese Journal of Automotive Engineering*, vol. 9, no. 3, pp. 182–192, 2019.

[34] K. Wei, Y. Yang, H. Zuo, and D. Zhong, "A review on ice detection technology and ice elimination technology for wind turbine," *Wind Energy*, vol. 23, pp. 433–457, 2020.

[35] H. Zuo, G. Liu, J. E et al., "Catastrophic analysis on the stability of a large dish solar thermal power generation system with wind-induced vibration," *Solar Energy*, vol. 183, pp. 40–49, 2019.

[36] F. Zhang, G. Liao, J. E, J. Chen, and E. Leng, "Comparative study on the thermodynamic and economic performance of novel absorption power cycles driven by the waste heat from a supercritical CO_2 cycle," *Energy Conversion and Management*, vol. 228, article 113671, 2021.

[37] H. Zuo, J. Tan, K. Wei, Z. Huang, D. Zhong, and F. Xie, "Effects of different poses and wind speeds on wind-induced vibration characteristics of a dish solar concentrator system," *Renewable Energy*, vol. 168, pp. 1308–1326, 2021.

[38] Q. Peng, W. Yang, J. E et al., "Investigation on H_2/air combustion with C_3H_8 addition in the combustor with part/full porous medium," *Energy Conversion and Management*, vol. 228, article 113652, 2021.

[39] D. Han, J. E, Y. Deng et al., "A review of studies using hydrocarbon adsorption material for reducing hydrocarbon emissions from cold start of gasoline engine," *Renewable and Sustainable Energy Reviews*, vol. 135, article 110079, 2021.

[40] H. Chu, Y. Ya, X. Nie, F. Qiao, and E. Jiaqiang, "Effects of adding cyclohexane, *n*-hexane, ethanol, and 2,5-dimethylfuran to fuel on soot formation in laminar coflow *n*-heptane/iso-octane diffusion flame," *Combustion and Flame*, vol. 225, pp. 120–135, 2021.

[41] X. Zhao, J. E, G. Liao, F. Zhang, J. Chen, and Y. Deng, "Numerical simulation study on soot continuous regeneration combustion model of diesel particulate filter under exhaust gas heavy load," *Fuel*, vol. 287, article 119795, 2020.

[42] J. E, M. Zhao, Q. Zuo et al., "Effects analysis on diesel soot continuous regeneration performance of a rotary microwave-assisted regeneration diesel particulate filter," *Fuel*, vol. 260, article 116353, 2020.

[43] B. Zhang, H. Zuo, Z. Huang, J. Tan, and Q. Zuo, "Endpoint forecast of different diesel-biodiesel soot filtration process in diesel particulate filters considering ash deposition," *Fuel*, vol. 272, article 117678, 2020.

[44] G. Wu, X. Wang, S. Abubakar, Y. Li, and Z. Liu, "A realistic skeletal mechanism for the oxidation of biodiesel surrogate composed of long carbon chain and polyunsaturated compounds," *Fuel*, vol. 289, article 119934, 2021.

[45] Y. Xie, Q. Zuo, M. Wang et al., "Effects analysis on soot combustion performance enhancement of an improved catalytic gasoline particulate filter regeneration system with electric heating," *Fuel*, vol. 290, article 119975, 2021.

[46] Y. Xie, Q. Zuo, G. Zhu et al., "Investigations on the soot combustion performance enhancement of an improved catalytic gasoline particulate filter regeneration system under different electric heating powers," *Fuel*, vol. 283, article 119301, 2021.

[47] J. E, M. Pham, D. Zhao et al., "Effect of different technologies on combustion and emissions of the diesel engine fueled with biodiesel: a review," *Renewable and Sustainable Energy Reviews*, vol. 80, pp. 620–647, 2017.